Transforming chaos to periodic oscillations

G. Kociuba,* N. R. Heckenberg, and A. G. White
Department of Physics, University of Queensland, St. Lucia, Queensland, Australia
(Received 30 November 2000; revised manuscript received 3 April 2001; published 24 October 2001)

We demonstrate that the dynamics of an autonomous chaotic class C laser can be controlled to a periodic state via external modulation of the pump. In the absence of modulation, above the chaos threshold, the laser exhibits Lorenz-like chaotic pulsations. The average amplitude and frequency of these pulsations depend on the pump power. We find that there exist parameter windows where modulation of the pump power extinguishes the chaos in favor of simpler periodic behavior. Moreover we find a number of locking ratios between the pump and laser output follow the Farey sequence.

DOI: 10.1103/PhysRevE.64.056220 PACS number(s): 05.45.−a, 03.65.Ta, 42.50.Dv, 03.67.−a

I. INTRODUCTION

In nonlinear systems with two degrees of freedom one parameter must be modulated in order to generate a third degree of freedom, thus allowing chaos to emerge. Many laser chaos experiments are performed this way [1]. Alternatively if a system already has three degrees of freedom, then chaos can emerge *without* modulation. The Lorenz-like chaos in the ammonia laser is an example of such autonomous chaos [2].

Dynamics of such chaotic systems have been studied both theoretically [3–5] and experimentally [6,7]. However, relatively little work has been done in investigating the properties of an autonomous chaotic system where one of the parameters is made time dependent [8]. This can either increase the complexity of the dynamics or simplify it. One mechanism for controlling autonomous chaos is to periodically cross the chaos threshold by varying the pump power [5,7]. However, this mechanism obviously cannot be used to control chaos if the system is permanently above the chaotic threshold. It is well known that a chaotic attractor is wound around a set of unstable periodic orbits [9]. This has led to the development of algorithms such as the Ott-Grebogi-Yorke (OGY) method [10] to select these orbits and control them. This requires detailed knowledge of the dynamical system, for example, an accurate estimate of the directions of the unstable and stable manifolds, in order to estimate how much change should be applied to a parameter in order to gain control. Thus the OGY algorithm is suitable for slow oscillating systems, but the required computation rapidly becomes intractable for fast oscillating systems.

Other feedback methods require no knowledge of the system Examples include occasional proportional feedback in a Nd:YAG pumped KTP crystal forming a multimode autonomous laser [11], and in a diode pumped Nd-doped silica fibre multimode autonomous laser [12]. Control by subtractive feedback has been shown in a nonautonomous CO_2 laser [13] and an autonomous NH_3 laser [14]. These systems require *a priori* knowledge of the average period of the chaotic pulsations, and a subtraction of the measured time series from its value at an earlier time.

Since these methods may not always be appropriate, we experimentally explore an alternative approach, which consists of applying a modulation to one of the parameters of the dynamical system. This changes the original system, but for a sufficiently small modulation, the unstable periodic orbits are similar to the corresponding orbits in the unmodulated system. Stabilizing one of these orbits should give control as predicted by theoretical studies [4,9,15,16].

To date, only class A and B lasers have been used in optical studies of control of chaos by modulation. For example, a nonautonomous class B laser was controlled by a small modulation of the losses to a periodic state [17]. Subharmonics of the pump were observed and three different locking ratios were found. Control of a class B multimode autonomous laser was found by modulating the pump [18]. In all cases the controlled output contained higher harmonics of the pump. A large range of locking ratios were found and chaos was almost suppressed to a dc level when the modulation frequency was above 25% of the fundamental pulsation frequency. It is interesting that a larger modulation of the pump was required to control the dynamics compared to modulation of the loss in the case of a multimode solid state laser [19].

Here, we use a chaotic class C laser, which has previously been shown to be well described by the complex Lorenz equations [20]. Previous numerical studies of these equations include modulation of the inversion across the bifurcation point [21], replacing the Rayleigh parameter with a time dependent term [15], and modulation of the inversion above the bifurcation point for the real Lorenz equations (corresponds to a nondetuned laser) [3]. Elsewhere we extend the latter model to include detuning [22]. It is this system which we explore here.

We find that there are many regions in modulation amplitude and modulation frequency parameter space, that cause the dynamics of the chaotic laser to frequency lock to the external periodic modulation, which form Arnold tongues and the locking ratio is rational. We show that a chaotic laser can be controlled to period q when modulated at period p, and the fractions p/q belong to the Farey sequence as was found in a nonchaotic laser [23] and in a bimode laser with a saturable absorber [24]. We find that these Arnold tongues are very narrow.

II. EXPERIMENT

Our system consists of $^{15}NH_3$ ring laser which is optically pumped by a $^{13}CO_2$ laser through a vibrational transition at

*Electronic address: kociuba@physics.uq.edu.au

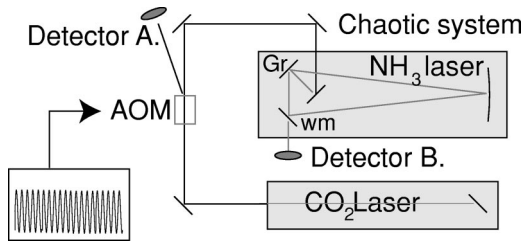

FIG. 1. Experimental schematic: CO_2 laser is the pump, NH_3 ring laser is the chaotic system, Gr is a blazed grating at the pump wavelength (10.78 μm) which doubles as a mirror for the lasing wavelength (153μm), wm is a wire mesh used as an output coupler, AOM is an acousto-optic modulator, detector A monitors the pump dynamics, and detector B monitors the FIR dynamics.

10.78 μm. The lasing occurs through a rotational transition at a wavelength 0.153 mm. We use a semiconfocal ring cavity as shown in Fig. 1, to achieve unidirectional lasing, where the backward traveling wave is chosen in preference to the forward wave because the ac. Stark effect splits the gain line in the forward direction [25].

Dynamics are optionally imposed on the pump by passing the laser beam though an acousto-optic modulator (AOM). The signal applied to the AOM is programmed using an arbitrary function generator. We monitor the CO_2 intensity via the first diffracted order from the AOM. This is detected by a $Hg_xCd_{1-x}Te$ photodetector A. The dynamics of the far infrared laser are observed by detecting the intensity of the output field with a fast Schottky barrier diode detector B, see Fig. 1. The signals from both detectors are recorded simultaneously onto a digital storage oscilloscope.

III. EXPERIMENTAL RESULTS

A. Harmonic pump modulation, harmonic generation–control to period 1

In general, modulation of the pump leads to no noticeable simplification in the dynamics. However, we have been able to identify a number of cases where, for specific ranges of modulation frequency and amplitude, periodic pulsations replace the chaotic spiking. Four cases are presented. Because the parameter ranges where periodic behavior can be observed are narrow, special care had to be taken to overcome the effects of unavoidable drifts during the experiment. Only then was it possible to distinguish consistent and reproducible patterns of behavior.

We apply a modulation to the pump of the form $f(t) = A[1+\sin(\omega t)]$ rather than $f(t) = A\sin(\omega t)$, so that we can be sure modulation occurs above the chaos threshold. This wave form is programmed into an arbitrary function generator which in turn modulates the AOM. The frequency was chosen to be near the average pulsation frequency of the free running chaos f_0. The lower trace of Fig. 2 indicates the periods where pump modulation was applied. The modulation depth was 20% as shown on the right hand *y*-axis scale. The upper trace shows the response of the FIR laser to this modulation. In order to display a time period much longer than the time between individual pulses, only the maximum

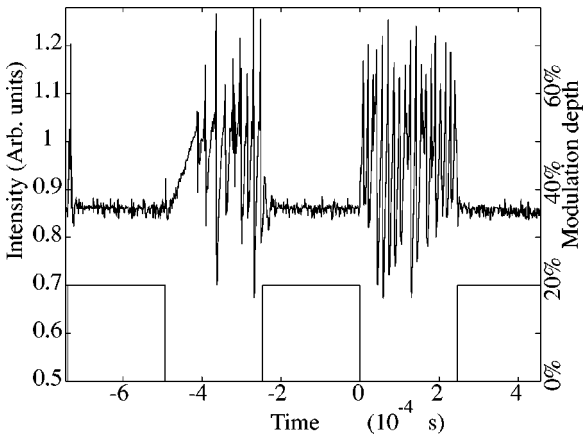

FIG. 2. Control to period 1. The lower trace is a schematic of the dynamics applied to the pump. The blocks of height 20% represent the period where pump modulation is applied (the modulation depth is shown on the right hand *y* axis). The upper trace is the *peak* output intensity of the pumped laser (intensity is shown on the left hand axis). As this is peak intensity, the flat regions represent period 1 pulsations.

pulse height is displayed, so that a horizontal line represents periodic pulses and each spike represents a Lorenz ''spiral'' of several successive pulses of increasing amplitude.

When modulation is applied, it is clear that the dynamics of the FIR laser has been transformed and is no longer chaotic. Figure 3(a) is an expanded view of one of the segments from Fig. 2. This shows that the Lorenz-like chaotic pulsations exist before modulation is applied to the system, and a period one signal develops as modulation is applied. The Fourier transform is calculated for the unmodulated laser output, and modulated output from Fig. 3(a), and shown as the upper trace, and lower trace, respectively, of Fig. 3(b). The initially chaotic system possesses a broad spectrum (gray), with three broadened harmonics of the fundamental pulsation frequency. This collapses to a set of sharp well defined harmonics with the fundamental located at the position of the fundamental pump modulation frequency. This shows the transformation from chaos to period 1 pulsations.

In Fig. 4 we examine these spectra more closely. Figure 4(a) is the spectrum of the FIR laser under modulation and Fig. 4(b) that of the pump. Higher harmonics of the fundamental are present even though there are only three evident harmonics associated with the pump. This may be that the laser is amplifying the pump harmonics, or that output harmonics are generated from a single pump modulation frequency, of some combination of both.

To analyze the effect of pump modulation on the FIR laser, we take the ratio of the spectrum during modulation, to the spectrum without, as shown in Fig. 4(c). A dashed line is added at the 0 dB level to differentiate attenuation and enhancement. It is clear that most frequencies have been attenuated whilst only the harmonics of the pump modulation frequency have been enhanced.

As the laser is initially chaotic before control was applied, we expect that the dynamics of the system does not immediately change from a chaotic state to a periodic state at the turn-on of the modulation, but does so after a few cycles of

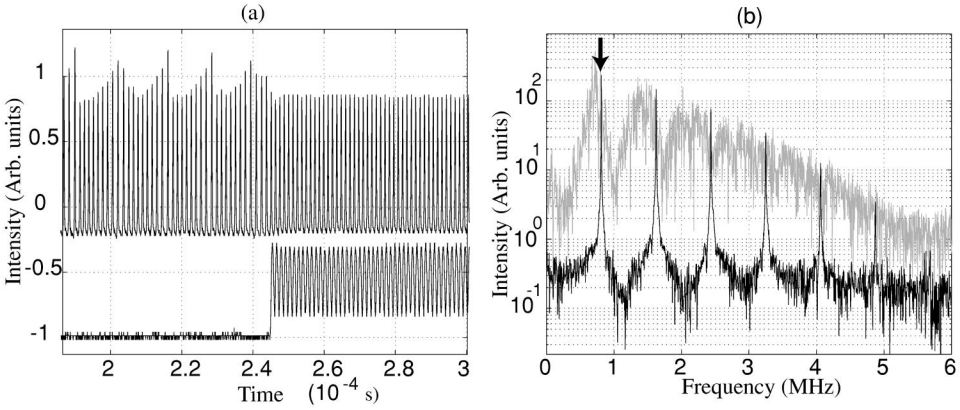

FIG. 3. Expanded view from -0.23 ms to 0 ms of Fig. 2. (a) Top trace is the intensity of the NH_3 laser output, lower trace is the pump intensity (the modulation depth between 0.25 ms and 0.3 ms is 20%). (b) Frequency spectra of the left (right) hand side of the NH_3 intensity trace from (a) are shown as the gray (black) trace. Note that the broad spectrum of the unmodulated case is transformed into a harmonic spectrum in the modulated case. The arrow indicates the position of the fundamental pump modulation frequency.

irregular behavior. This is most clearly seen by performing the following experiment. The laser was modulated at f_0 to give period 1, then allowed to return to its chaotic state (by removing the modulation), finally the same modulation was applied to the laser thus resulting in period 1. Figure 5 this sequence of events, allows the laser to develop different initial conditions between the first and second modulation period of control. Figure 6 shows the intensity outputs from both periods. The solid line is the response to the first modulation, while the dashed line is the response to the second. Both these lines are different between time zero and 0.014 ms, since at this interval both intensities are not phased locked to the pump modulation. After 0.014 ms, both these intensities are phased locked, hence the two curves in the graph of Fig. 6 collapse onto the phase locked curve.

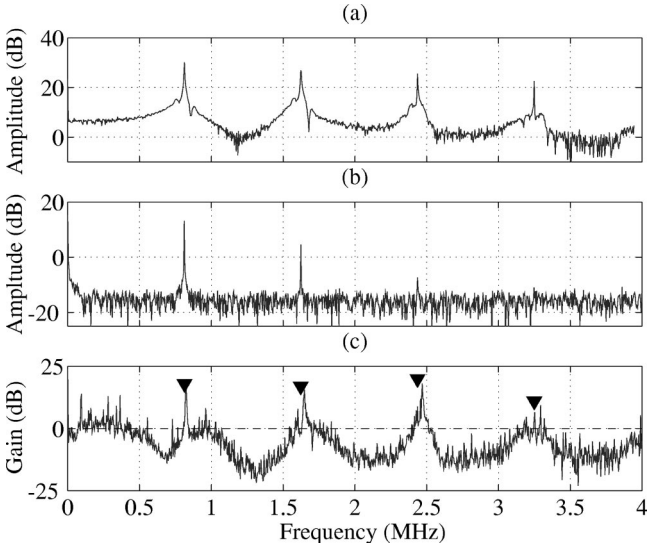

FIG. 4. Fourier spectra for (a) the pump modulated FIR laser output, (b) the pump modulation, and (c) the ratio of the pump modulated FIR laser output to the unmodulated laser output. Triangles indicate the position of the integer harmonics. the dashed line indicates the position of zero gain, note that only the harmonics of the pump are amplified, all other frequencies are suppressed.

Experimentally, control to period 1 could be observed over a narrow range of pump modulation frequency and amplitude. Changing any one of the parameters by 1% is enough to destroy control. Clearly, experimental drift issues would need to be addressed before undertaking a full map of the parameter space, but these results are enough to show that while control is possible, it is not easy to achieve.

B. Harmonic pump modulation, subharmonic generation–control to period 3

We also found that it is possible to control states to higher integer periods (e.g., pattern repeats every three pulses). Figure 7 is similar to Fig. 3(a) except now we have lowered the pump modulation frequency by 16%. It shows that the laser takes many cycles before it settles down to period 3 pulsations, and that the period 3 behavior is not perfectly regular. We believe this is due to the sensitive dependence on modulation frequency relative to the natural pulsation frequency of the ammonia laser which in turn depends on the frequency and power of the pump laser, both which are subject to jitter and drift. In the frequency domain it is clear that the dynamics of the laser has been simplified, as is evident in Fig. 8. The frequency spectrum for the FIR laser output is shown on the upper trace, and the pump spectrum on the lower trace. Note that we are pumping near the fundamental frequency f_0, and we generate rational subharmonics at $\frac{1}{3}\ f_0$ and $\frac{2}{3}\ f_0$, indicated by f_1 and f_2 in Fig. 8, which are not present in the pump. Higher harmonics such as $\frac{4}{3}\ f_0$ and $\frac{5}{3}\ f_0$ are present as well as integer multiples of all rational harmonics.

We found that the laser output contains harmonics of the pump when the modulation frequency was chosen to be

FIG. 5. Schematic of modulation applied to the pump. The pump is modulated at f_0, the fundamental pulsation frequency, for 100 cycles between a and b, followed by a period of no modulation between b and c, followed by 100 cycles at f_0 between c and d.

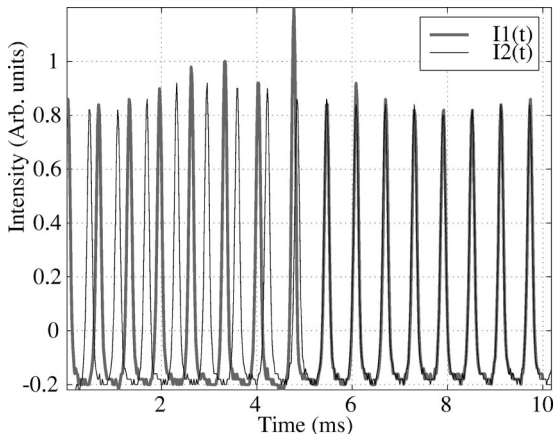

FIG. 6. Two intensity outputs of the laser corresponding to modulation of the pump to give period 1. The solid line is the response to modulation at f_0, while the dashed line also is a response to the same modulation, but applied after the system was allowed to return to its chaotic state. Therefore the difference between the two traces is the initial conditions.

about 10% higher than f_0. However, if we bring the modulation frequency to within a few percent of f_0, we find that subharmonics emerge in addition to the pump harmonics.

C. Subharmonic pump modulation, subharmonic generation–control to period 1

Consider the chaotic spectrum of Fig. 3. The results of the last two sections were obtained by modulating at a frequency near to the first peak of the chaotic spectrum f_0. If we instead modulate at half this frequency, Fig. 9 shows the result. There is transient behavior for approximately 20 cycles before the FIR laser output is controlled to period 1 at f_0. This is clearer in the associated frequency spectrum shown in Figs. 10(a) and 10(b). As previously, there are sharp well defined harmonic peaks in the FIR laser output spectrum which shows periodic behavior. However, now the main pulsation frequency of the laser is at twice the pump modulation frequency. Figure 10(c), the ratio of the modulated to the

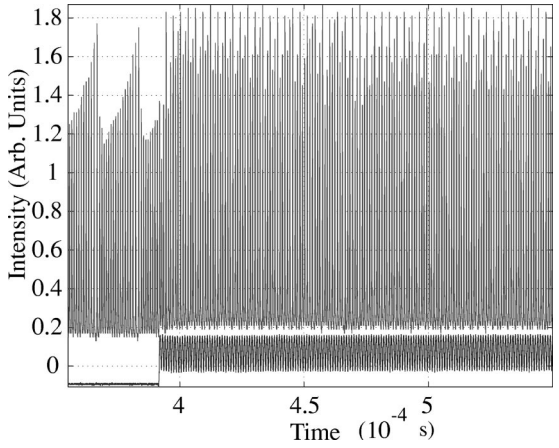

FIG. 7. Control to period 3 after many pulses of instability. Same conditions as Fig. 3(a) except that the modulation frequency is lowered by 16%.

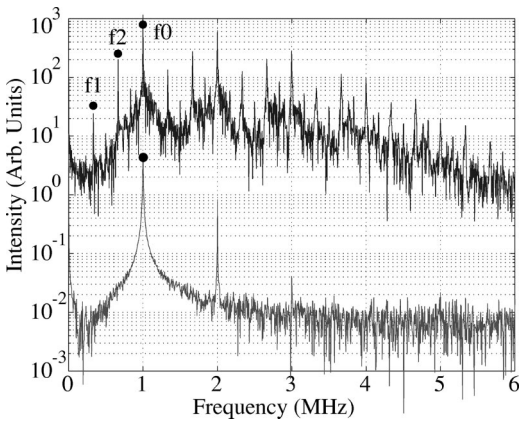

FIG. 8. Control to period 3. Lower trace is the frequency spectra of the pump where the modulation frequency is indicated by a dot. The upper trace is the frequency of the FIR laser during modulation. f_0, f_2, f_1 indicate the fundamental pulsation frequency f_0, and the rational subharmonics $\frac{2}{3}f_0$, and $\frac{1}{3}f_0$, respectively. Note the presence of higher harmonics of these frequencies.

unmodulated spectra, shows that the enhancement of $\frac{1}{2}f_0$ (located at 0.4 MHz) is slightly larger than at f_0. However, the time trace in Fig. 9 clearly shows the main pulsation frequency to be at f_0, not at $\frac{1}{2}f_0$. This is evident in the FIR output spectrum in Fig. 10(a) since the signal at f_0 is larger than at $\frac{1}{2}f_0$ due to the fact that the baseline at f_0 is higher than at $\frac{1}{2}f_0$. This suggests that the mechanism for control could be that the unstable periodic orbit at $\frac{1}{2}f_0$ has been stabilized, or that the second harmonic of the pump, is stabilizing the unstable periodic orbit f_0 of the FIR laser. The presence of these two harmonics in the pump dynamics makes this distinction ambiguous.

D. Subharmonic pump modulation subharmonic generation–control to other periods

We now look for locking ratios other than 1/1 with the aim of stabilising any other unstable periodic orbits that may exist. We do this by systematically stepping through modulation frequency with a fixed amplitude to search for periodic solutions. Figure 11 is a graphical description of this experi-

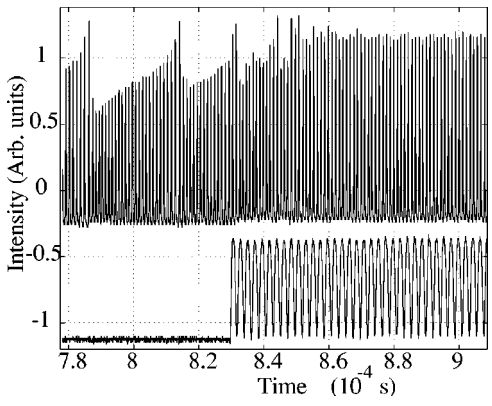

FIG. 9. Control to period 1 from an initially chaotic state. Upper trace is the FIR laser intensity output, lower trace is the modulation applied to the pump at $\frac{1}{2}f_0$.

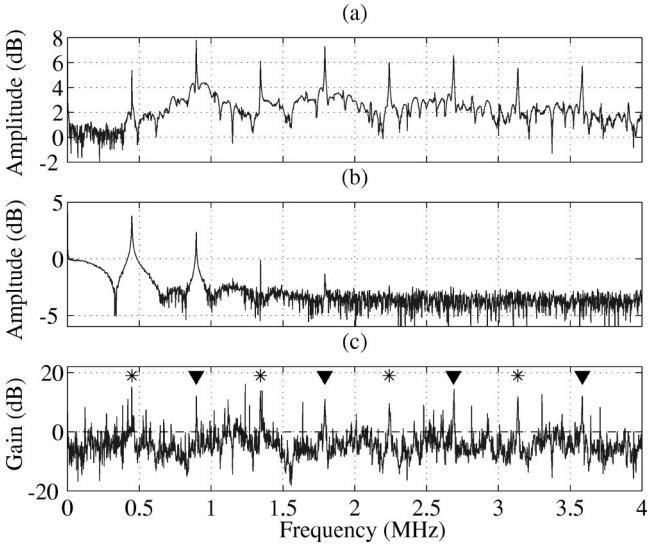

FIG. 10. Fourier spectra for (a) the pump modulated FIR laser output, (b) the pump modulation and (c) the ratio of the pump modulated FIR laser output to the unmodulated laser output. Triangles indicate the position of the integer harmonics. the dashed line indicates the position of zero gain, note that the harmonics and subharmonics of the pump are amplified, all other frequencies are suppressed.

ment. The lower trace shows the variations in pump power imposed by the AOM. We fix the amplitude and reduce the frequency of modulation in five discrete steps each of which last about 100 cycles. These are separated by unmodulated periods lasting the same amount of time. This is schematically shown as sine waves separated by horizontal lines in Fig. 11. This sequence is sandwiched between two ramp functions. The purpose of the ramp is to locate the chaos threshold for the laser system, which was used to check that

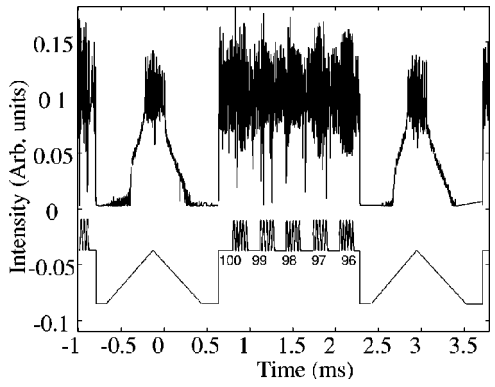

FIG. 11. The lower trace represents the dynamics applied to the pump. This consists of a triangle wave form of low frequency, followed by five sinusoidal wave forms labeled 100, . . . ,96 with relative frequency 100, . . . ,96, respectively, followed by another slow triangle wave form. The triangle wave form is used as a diagnostic to locate the chaos threshold. The five sine waves represent a systematic step through the frequency parameter at fixed amplitude. This gives us information on how close controlled orbits are in frequency, and the width of control. The upper trace is FIR laser output where only the maximum intensity peaks are displayed. 11

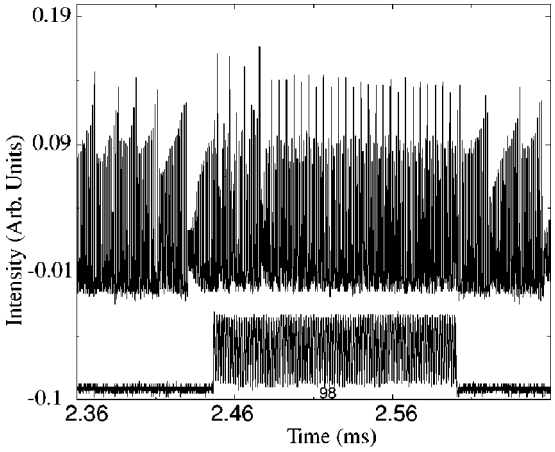

FIG. 12. Expanded view of third modulation segment labeled ''98'' in Fig. 11. This shows period 4 pulsations exist after 32 irregular pulses after the application of modulation.

the modulation sequence remained above the chaos threshold in spite of any parameter drift. The upper trace shows the FIR laser response to these events. For display purposes only the maximum pulse height is shown.

The first modulation applied in the sequence is labeled ''100.'' The dynamics shown in the upper trace is no longer Lorenz-like but more complicated. (This is not apparent in Fig. 11 because of aliasing in the printing.) As the frequency is reduced (99) the dynamics is still not simplified, however, there is a small section in the time series where the signal is period 4 before complicated dynamics takes over. When the frequency is reduced further (98) there is a small period of transient behavior at the start of the modulation but the intensity quickly settles down to period 4 pulsations and remains there until the modulation is turned off. This is shown in more detail in Fig. 12. Decreasing the modulation frequency further (97) destroys any period 4 behavior in favor of complicated dynamics, although there now is a small section in the time series where period 7 emerges, but does not persist for the modulation duration. Finally, decreasing the frequency by one more step (96) results in the intensity following a period 7 orbit after a relatively short initial irregular behavior. These results are typical. It is instructive to analyze the dynamics of the system by constructing a Lorenz map from the intensity data. This is a plot of the peak intensity of a pulse against the peak intensity of the previous pulse [26]. For a Lorenz-like chaotic system a cusp shaped curve is traced out [27]. Figure 13 shows the Lorenz Maps of the chaotic system (a) without modulation and (b) with modulation for the period 4 case. Without modulation there is the characteristic cusp shape indicative of chaos. With modulation four definite regions become apparent. All points are connected by lines to give time ordering information, so that periodic behavior can be easily distinguished from a nonperiodic signal or chaos, since a period *n* signal will appear as an *n*-sided polygon. The lines outside this polygon are due to the transient behavior before control. This metastable behavior is due to the nonperfect intersection of the attractor corresponding to the unmodulated chaotic laser, with the attractor of the modulated laser, and the weak stability of the new attractor as discussed earlier. Sampling error and detector

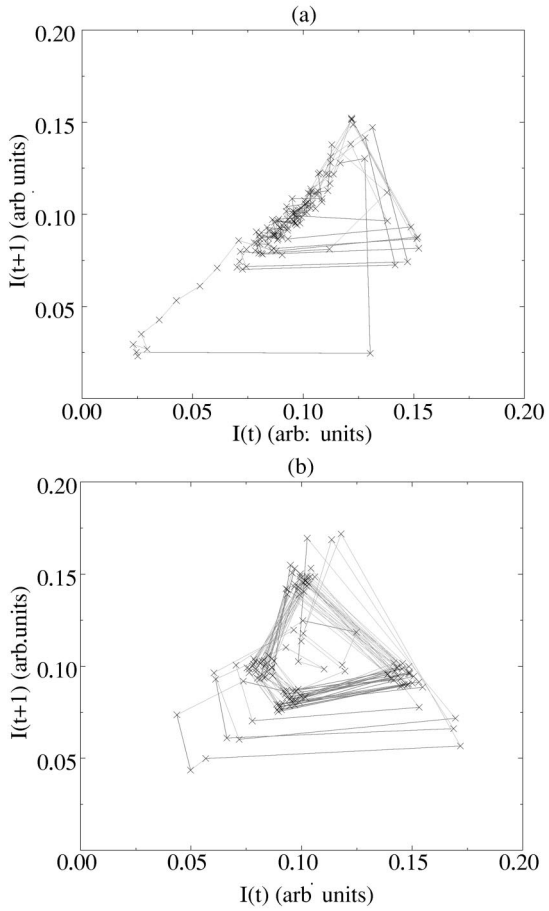

FIG. 13. Lorenz maps of the FIR laser output are constructed from Fig. 12. (a) Without modulation and (b) with modulation. The cusp shape in (a) is characteristic of Lorenz-like chaos. The polygon shape of (b) when the points are joined shows period four pulsations.

noise cause the four points of the polygon to have some spread from an ideal polygon generated from noiseless points. Figure 14(a1) and 14(b1) are the spectra of the modulated FIR laser for period 4 and 7, respectively. The associated pump spectra are shown on plots (a2) and (b2).

A similar sequence of modulation was applied to the pump which resulted in the generation of a period 6 orbit shown in Figure 15. The frequency spectra of the modulated pump and laser output is shown on Figure 16. It is clear that the pump modulation frequency is not on the fundamental pulsation frequency of the laser output f_0, but at $\frac{5}{6}f_0$.

These results show that the fundamental pulsation frequency of the FIR laser f_0 does not coincide with any of the harmonics of the pump, since control to period 4, 6, and 7 required a modulation frequency of $\frac{3}{4}f_0$, $\frac{5}{6}f_0$, and $\frac{5}{7}f_0$, respectively. From the time domain we know that the pump modulation and the FIR laser output are phase locked. This shows that there are three more Arnold tongues with locking ratios 3:4, 5:6, and 5:7, respectively. For the real Lorenz equations, locking ratios of the form $(l\text{-}1)\text{:}l$ and $(l\text{-}2)\text{:}l$ were predicted for $l>10$ [3]. In our case l was 3, 4, and 5, respectively.

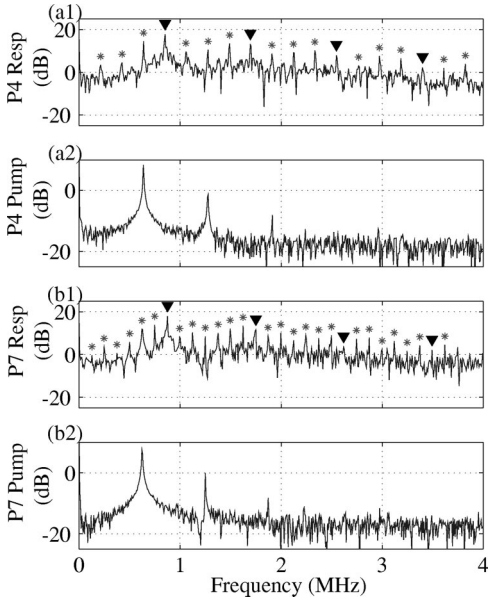

FIG. 14. Fourier spectra for two different harmonic generation experiments: (a1) and (b1) are the spectra of the FIR laser during modulation to give periods 4 and 7 respectively. The corresponding dynamics applied to the pump are shown in (a2) and (b2), respectively. The triangles indicate the position of the integer harmonics, while the stars indicate rational harmonics. In both cases the maximum peak in the FIR spectra correspond the the fundamental pulsation frequency of the unmodulated chaos.

It has been found that the dependence of the locking ratios on a control parameter forms a Devil's staircase in the circle map [28] and in the Bonhoeffer Van der Pol model [29], and is considered to be a universal phenomena. The Devil's staircase is made up of rational numbers belonging to the Farey sequence. That is, given two locking ratios p/q and r/s there can be another locking ratio of $(p+r)/(q+s)$ restricted to $|ps-qr|=1$. We have found six of these locking ratios 1:1, 1:2, 1:3, 3:4, 5:6, and 5:7. These lie on six stairs of the Devil's staircase on a graph of locking ratio against modulation frequency. We cannot explicitly assign lengths to each of these stairs as the modulation frequency could only be altered in discrete steps (1%). To get an estimate of the lengths of each of the stair we return to the experimental data summarized in Fig. 11. The segments labeled (99) and (97) show windows of period 4 and period 7, respectively, before complicated dynamics takes over as mentioned earlier. This is not a simple phase slip of the period 4 and period 7 orbits, as can occur at the boundary of an Arnold tongue [30]. Therefore these two segments lie outside the Arnold tongues, thus we can be sure that the width of these tongues are less than 1% for a modulation depth of 20%. The period 4 and period 7 orbits which briefly appear are the result of the trajectories in phase space finding a period 4 and period 7 saddle orbit. The trajectories follow the stable manifold for a few periodic cycles before the unstable manifold of the saddle orbit takes effect and repels it to another torus. Therefore we know the lengths on the stairs in the Devil's staircase of our data would have an upper bound of 1% of the modulation frequency, and a nonzero lower bound since these ex-

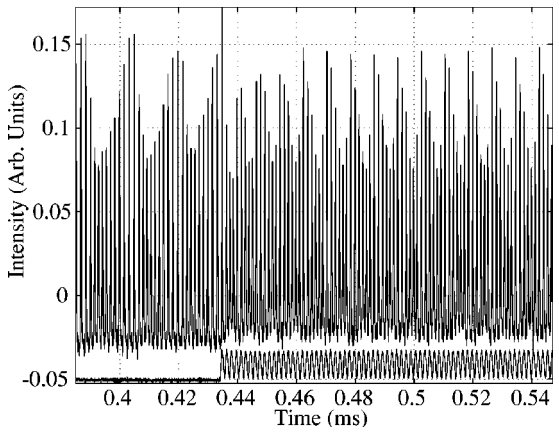

FIG. 15. Control to period 6. The lower trace is the pump and the upper trace is the FIR laser output.

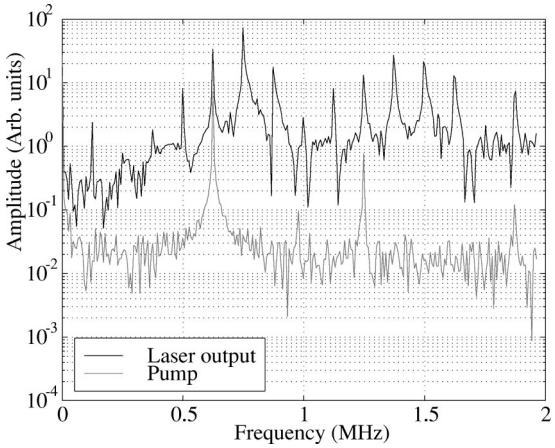

FIG. 16. Control to period 6. The lower trace is the frequency spectra of the pump during modulation and the upper trace is the frequency of the FIR laser during modulation.

periments were repeatable. Thus the narrow width of modulation frequency required to give control strongly suggests that resonance is taking place, that is the mechanism for control is likely to be stabilization of the unstable periodic orbit in the modulated system.

Experimental difficulties such as drift of the laser parameters and discreteness of modulation frequency it is difficult to locate the positions of each stable island in the parameter space. Elsewhere we present a theoretical treatment that enables a more systematic exploration of the number and structure of these islands in control parameter space [22].

IV. CONCLUSION

We have demonstrated experimentally that a class C laser can be controlled to a periodic state even though it is driven above the chaos threshold, by applying an appropriate modulation frequency to the pump. It is also possible to modulate the pump at the fundamental pulsation frequency of the chaotic laser to generate not only integer harmonics of the pump, but also rational harmonics that are not present in the pump modulation frequency. We have also shown that control is not restricted to modulating at the harmonics of the fundamental pulsation frequency, as pumping at rational values of the harmonic, according to specific values of the Farey sequence, also gave control. We therefore expect there are other locking ratios which could give control. We found that the Arnold tongues were close together but they did not overlap thus allowing control to a unique period for particular parameter values. The width of the tongues in frequency space is very narrow, since changing any parameter of the order of 1% destroyed control. It is likely that the mechanism for control is stabilization of one of the existing closely spaced unstable periodic orbits in the modulated system.

[1] R. Roy and K. S. Thornburg, Jr., Phys. Rev. Lett. **72**, 2009 (1994).
[2] C. Weiss and W. Klische, Opt. Commun. **51**, 47 (1984).
[3] E.-H. Park, M. A. Zaks, and J. Kurths, Phys. Rev. E **60**, 6627 (1999).
[4] Y. Braiman and I. Goldhirsch, Phys. Rev. Lett. **66**, 2545 (1991).
[5] H. Zeghlache and P. Mandel, J. Opt. Soc. Am. B **2**, 18 (1985).
[6] D. Y. Tang, R. Dykstra, M. Hamilton, and N. R. Heckenberg, Phys. Rev. E **57**, 3649 (1998).
[7] R. Dykstra, A. Rayner, D. Y. Tang, and N. R. Heckenberg, Phys. Rev. E **57**, 397 (1998).
[8] W. X. Ding, H. Q. She, W. Huang, and C. X. Yu, Phys. Rev. Lett. **72**, 96 (1994).
[9] J. P. Eckmann and D. Ruelle, Rev. Mod. Phys. **57**, 617 (1985).
[10] E. Ott, C. Greborgi, and J. A. Yorke, Phys. Rev. Lett. **64**, 1196 (1990).
[11] R. Roy, J. T. W. Murphy, T. D. Maier, and Z. Gills, Phys. Rev. Lett. **68**, 1259 (1992).
[12] S. Bielawski, D. Derozier, and P. Glorieux, Phys. Rev. A **47**, R2492 (1993).
[13] S. Bielawski, D. Derozier, and P. Glorieux, Phys. Rev. E **49**, R971 (1994).
[14] R. Dykstra, D. Y. Tang, and N. R. Heckenberg, Phys. Rev. E **57**, 6596 (1998).
[15] J. Bhattacharjee, K. Banerjee, D. Chowdhury, and R. Saravanan, Phys. Lett. **104A**, 33 (1984).
[16] K. A. Mirus and J. C. Sprott, Phys. Rev. E **59**, 5313 (1999).
[17] M. Ciofini, R. Meucci, and F. T. Arecchi, Phys. Rev. E **52**, 94 (1995).
[18] M. Kang, K. Cho, C. Kim, S. Gil, and J. Lee, J. Opt. Soc. Am. B **15**, 2410 (1998).
[19] P. Colet and Y. Braiman, Phys. Rev. E **53**, 200 (1996).
[20] C. Weiss, R. Vilaseca, N. Abraham, R. Corbalan, E. Roldan, and G. de Valcarcel, Appl. Phys. B: Lasers Opt. **61**, 223 (1995).
[21] T. Ogawa and E. Hanamura, Appl. Phys. B: Photophys. Laser Chem. **43**, 139 (1987).

[22] G. Kociuba and N. R. Heckenberg (unpublished).
[23] D. Baums, W. Elsasser, and E. Gobel, Phys. Rev. Lett. **63**, 155 (1989).
[24] D. Hennequin, D. Dangoisse, and P. Glorieux, Phys. Rev. A **42**, 6966 (1990).
[25] G. Willenberg, J. Heppner, and G. Schinn, IEEE J. Quantum Electron. **QE-18**, 2060 (1982).
[26] E. N. Lorenz, J. Atmos. Sci. **20**, 130 (1963).
[27] M. Y. Li and N. R. Heckenberg, Opt. Commun. **108**, 104 (1994).
[28] M. Jensen, P. Bak, and T. Bohr, Phys. Rev. Lett. **50**, 1637 (1983).
[29] S. Yasin, M. Friedman, S. Goshen, A. Rabinovitch, and R. Thieberger, J. Theor. Biol. **160**, 179 (1993).
[30] A. Pikovsky, G. Osipov, M. Rosenblum, M. Zaks, and J. Kurths, Phys. Rev. Lett. **79**, 47 (1997).